Procedures to Improve the Accuracy of Airborne Doppler Radar Data

BRIAN L. BOSART*

Department of Atmospheric Sciences, University of California, Los Angeles, Los Angeles, California

WEN-CHAU LEE

National Center for Atmospheric Research,+ Boulder, Colorado

ROGER M. WAKIMOTO

Department of Atmospheric Sciences, University of California, Los Angeles, Los Angeles, California

(Manuscript received 12 December 2000, in final form 22 May 2001)

ABSTRACT

The navigation correction method proposed in Testud et al. (referred to as the THL method) systematically identifies uncertainties in the aircraft Inertial Navigation System and errors in the radar-pointing angles by analyzing the radar returns from a flat and stationary earth surface. This paper extends the THL study to address 1) error characteristics on the radar display, 2) sensitivity of the dual-Doppler analyses to navigation errors, 3) fine-tuning the navigation corrections for individual flight legs, and 4) identifying navigation corrections over a flat and nonstationary earth surface (e.g., ocean).

The results show that the errors in each of the parameters affect the dual-Doppler wind analyses and the first-order derivatives in different manners. The tilt error is the most difficult parameter to determine and has the greatest impact on the dual-Doppler analysis. The extended THL method can further reduce the drift, ground speed, and tilt errors in all flight legs over land by analyzing the residual velocities of the earth surface using the corrections obtained in the calibration legs.

When reliable dual-Doppler winds can be deduced at flight level, the Bosart–Lee–Wakimoto method presented here can identify all eight errors by satisfying three criteria: 1) the flight-level dual-Doppler winds near the aircraft are statistically consistent with the in situ winds, 2) the flight-level dual-Doppler winds are continuous across the flight track, and 3) the surface velocities of the left (right) fore radar have the same magnitude but opposite sign as their counterparts of right (left) aft radar. This procedure is able to correct airborne Doppler radar data over the ocean and has been evaluated using datasets collected during past experiments. Consistent calibration factors are obtained in multiple legs. The dual-Doppler analyses using the corrected data are statistically superior to those using uncorrected data.

1. Introduction

Airborne Doppler radars have been extensively used in recent years for studying mesoscale events, such as supercells (e.g., Wakimoto et al. 1998; Wakimoto and Liu 1998), frontal systems (e.g., Wakimoto and Bosart 2000), drylines (e.g., Atkins et al. 1998), squall lines (e.g., Jorgensen et al. 1997), mesoscale convective systems (e.g., Chong and Bousquet 1999), and hurricanes (e.g., Marks et al. 1992). Analyzing airborne Doppler radar data is complicated by the fact that the radar is mounted on a moving platform. Hence, the measured Doppler velocities contain both a meteorological component and a platform motion component. For the National Center for Atmospheric Research's (NCAR) Electra Doppler Radar (ELDORA) or the National Oceanic and Atmospheric Administration's (NOAA) P3 tail Doppler radars, there are a total of nine parameters involved in computing the platform motion component and the coordinate transformation to map radar data onto an earth-relative coordinate system. Precisely removing the platform motion component from the measured Doppler velocities and mapping data onto an earth-relative coordinate system are the first two major steps toward creating an accurate dual-Doppler wind synthesis (Lee et al. 1994; Testud et al. 1995).

* While this paper was in press, Brian Bosart was killed in a tragic automobile accident. He was a graduate student nearing the completion of his Ph.D. thesis. This paper is published in his memory.

+ The National Center for Atmospheric Research is sponsored by the National Science Foundation.

Corresponding author address: Dr. Wen-Chau Lee, Atmospheric Technology Division, National Center for Atmospheric Research, Boulder, CO 80307-3000.
E-mail: wenchau@ucar.edu

It is known that there are errors/biases associated with these parameters resulting from the uncertainties in the aircraft Inertial Navigation System (INS), mounting and calibration errors in the radar systems, the physical separation between the INS and the radar antenna, flexibility (distortion) of the airframe, and other unknown error sources. These errors are reflected in the nine parameters resulting in errors in the Doppler velocities and their earth-relative position. Because of the nine degrees of freedom, it is difficult to separate the individual effects from these nine parameters. In contrast, a ground-based radar has only three degrees of freedom (azimuth angle, elevation angle, and range delay). Using stationary ground targets and solar calibration, these biases can be determined unambiguously. Previously, the errors associated with airborne radars have been identified empirically by examining the error characteristics in the Doppler velocity pattern. Then, a correction to each individual parameter is made to satisfy the criterion that the earth surface is flat and stationary (F. Marks 1999, personal communication). However, the signatures of these individual errors as they appear on the Doppler radar display have not been documented in the literature.

Testud et al. (1995; hereafter, referred to as THL) derived a systematic approach to identify these errors and biases from individual parameters by analyzing the returns of a flat and stationary earth surface as a function of antenna rotation angle. This variational procedure has performed well using the ELDORA data collected during the Tropical Ocean Global Atmosphere Coupled Ocean–Atmosphere Response Experiment (TOGA COARE; Webster and Lukas 1992) and has become a standard procedure at NCAR to identify and correct for the navigation and radar-pointing angle errors. Georgis et al. (2000) extended the THL method by including digitized topographic information as an additional constraint so it could be applied over complex terrain. Their method is able to resolve aircraft position errors (latitude and longitude) in addition to those standard parameters resolved in the THL method. A similar approach has been implemented by Durden et al. (1999) to correct the Doppler velocities from the platform motion in the Airborne Rain Mapping Radar on board the National Aeronautics and Space Administration DC-8.

Several issues remain unresolved in the above studies. First, both of these advanced methods can only be applied to a stationary earth surface. The THL method encountered difficulties when applied to the Fronts and Atlantic Storm Track Experiment (FASTEX; Joly et al. 1997) data where the ocean surface moved at least several meters per second. Second, the uncertainties in isolating the tilt angle, drift angle, and ground speed errors remained a problem. It takes significant time, experience, and effort to identify these three errors even using the advanced methods. In addition, the drift angle and ground speed corrections obtained from the calibration legs may not be applied to all flight legs. Third, the effect of an individual error on the radar display has not been documented. Last, the quantitative impact that these errors have on the dual-Doppler wind analysis has not been shown. It should be noted that the quality of the airborne dual-Doppler winds has been examined by statistically comparing the flight-level winds with the nearby dual-Doppler winds (Marks et al. 1992; Atkins et al. 1998). However, the effect of the navigation errors on the dual-Doppler wind analyses has not been demonstrated.

The purpose of this paper is threefold. First, present Doppler velocity signatures and the sensitivities of the dual-Doppler analysis owing to the errors in the individual parameters. Second, present the extended THL (ETHL) method to refine tilt, drift, and ground speed corrections to all flight legs over land. Third, propose and evaluate the Bosart–Lee–Wakimoto (BLW) method to determine the tilt, drift, and ground speed corrections in all surface conditions when extensive dual-Doppler radar winds can be deduced at the flight level on both sides of the aircraft. Section 2 presents a brief review of the THL method. Section 3 documents the Doppler velocity signatures on radar displays owing to the errors from individual parameters. Section 4 presents the sensitivities of the dual-Doppler winds and their first-order derivatives on these errors. The ETHL method to determine and refine the tilt, ground speed, and drift errors for all flight legs is presented in section 5. Section 6 discusses the BLW method to deduce the tilt, ground speed, and drift errors by statistically matching the flight-level dual-Doppler winds and in situ winds. Results are presented in section 7. A discussion and summary are, respectively, presented in sections 8 and 9. The necessary equations used in this paper are summarized in the appendix.

2. A review of the THL

As documented in THL and Lee et al. (1994), a total of nine parameters affect the accuracy of airborne Doppler radar data. Among these nine parameters, five [aircraft ground speed (V_H), drift angle (α), pitch angle (β), roll angle (γ), and aircraft vertical velocity (w)] are determined by the aircraft INS and/or the Global Positioning System. Three of the nine parameters are related to the radar system [tilt angle (θ), rotation angle (ϕ), and range delay (ΔR)]. The aircraft altitude (H) is determined from the radar altimeter or the pressure altitude. Hereafter, the parameters associated with an angle are omitted and are referred to as drift, pitch, roll, rotation, and tilt. Since the rotation and roll are defined with respect to the same spin axis around the fuselage for an airborne tail Doppler radar, their errors are not separable and are grouped together as a roll/rotation correction ($\delta\phi$) in the following discussion. Hence, the number of variables decreases from nine to eight. Note that for other airborne radar systems, the roll and rotation may be defined differently but will be affected

by these uncertainties. The definition of the parameters can be found in Lee et al. (1994) and THL.

If all parameters contain no errors and the aircraft motion is removed, a stationary and flat earth surface will appear horizontal and the surface residual velocities will be zero on a Doppler velocity display.[1] In most situations, however, these two criteria are not met. The THL method was designed to deduce a set of correction factors for the eight parameters in order to satisfy the flat and stationary earth surface criteria. By examining geometric relations in spherical coordinates, THL derived two sets of equations, the velocity equation and the range equation [(10) and (18) in THL], that govern the error characteristics of the eight parameters as a function of the rotation, ϕ. Key equations in THL are summarized in the appendix. All delta (δ) quantities are defined as the true value minus the measured value (THL). Therefore, all correction factors obtained in the THL procedure should be added to their corresponding measured value to yield the estimated true value.

A total of seven independent equations govern the eight parameters. These coefficients can be obtained via a least squares fit of the surface velocity residual and the distance residual on all available rotation angles of a single sweep. A sweep is defined as one complete rotation of a radar. THL suggested that these corrections be averaged over several minutes to reduce the sweep-by-sweep fluctuations of these corrections. There are five equations governing five parameters ($\delta\phi$, $\delta\beta$, δw, δH, and ΔR) where the THL method provides robust error estimates. It has become standard procedure for the THL method to first compute corrections for these five parameters then compute the drift, tilt, and ground speed corrections. THL assumed no errors in tilt as ''a priori'' in order to solve for the ground speed and drift errors. Note that the equations governing drift, tilt, and ground speed corrections form an underdetermined system. As a result, multiple sets of solutions for these three variables that meet the criteria of a flat and stationary earth surface may exist.

3. Error characteristics on a Doppler velocity display

The Doppler velocity patterns resulting from the error in each parameter are illustrated in this section using schematic diagrams and data collected during past field experiments. Interpretation of the error characteristics is presented here using geometric arguments. The error characteristics of a single parameter are illustrated by assuming all other parameters contain no error unless stated otherwise.

[1] Practically, it is only reasonable to expect the average velocity, not the velocity of the individual pixels, of the surface to be zero.

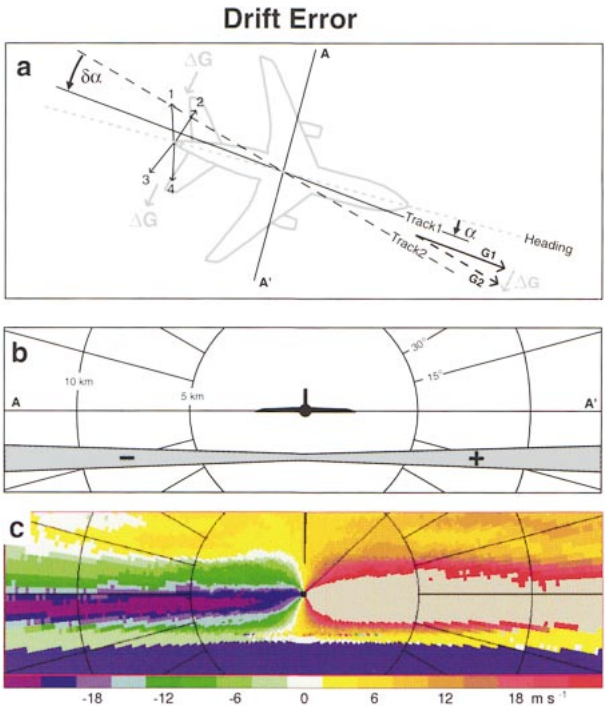

FIG. 1. Schematic diagrams of the Doppler velocity pattern due to a negative drift error ($\delta\alpha < 0$). (a) The plane view of the error vectors. The **G1** is the true ground speed vector (along track 1) while **G2** is the apparent ground speed vector (along track 2) measured by the INS. Here Δ**G** is the error velocity vector of the earth surface due to subtracting an incorrect **G2**. Horizontal positions for the fore (aft) radar are labeled 2 and 4 (1 and 3). (b) The illustration of the residual surface velocities appearing on the fore radar display on the AA′ cross section. The gray shades represent the earth surface. Plus (+) and minus (−) indicate the sign of the residual surface Doppler velocities. The aircraft is located at the center of the plot. (c) The corresponding radar display in (b) with observed data. Color scale shows the single Doppler velocities in m s^{-1}. Warm (cold) colors are Doppler velocities moving away (toward) the radar. Gray color in the figure represents Doppler velocities greater than 24 m s^{-1} (off the color scale).

a. The drift error ($\delta\alpha$)

Drift is the angle between the aircraft track (the footprint of the aircraft on the earth surface) and heading (the direction of the fuselage) as illustrated in Fig. 1a. The drift is positive when the track is shifted clockwise from the heading. The drift error is primarily from the uncertainty in determining the true heading and track[2] resulting from the two well-known sources of INS Schuler oscillation and inertial drift (Masters and Leise 1993). In Fig. 1a, **G1** is the true aircraft motion vector along the true track (labeled track 1) while **G2** is the

[2] The Honeywell manual for the INS system on the NCAR Electra lists an accuracy of 0.2° for the true heading. Track is computed from the ground speed that has a nominal 1 m s^{-1} uncertainty. This uncertainty translates to a 0.3° uncertainty in track assuming a 120 m s^{-1} ground speed.

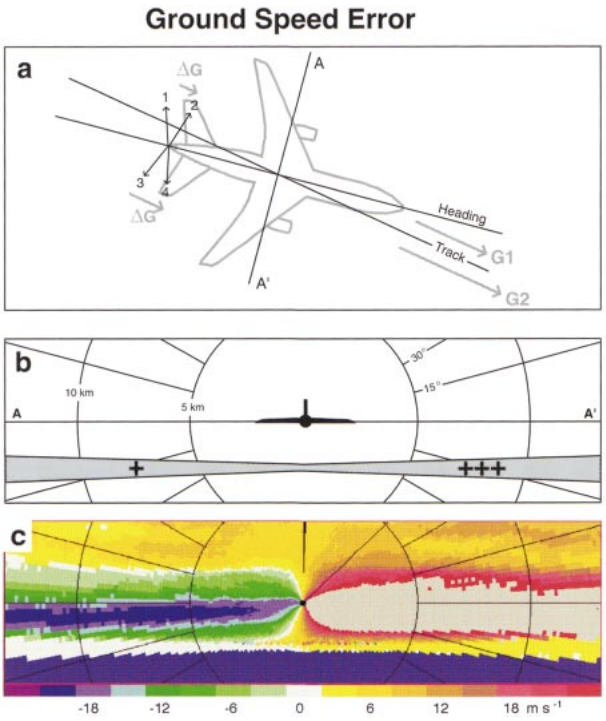

FIG. 2. Same as Fig. 1 but for a negative ground speed error. Here "+" and "+++" indicate the relative magnitude of the surface velocities.

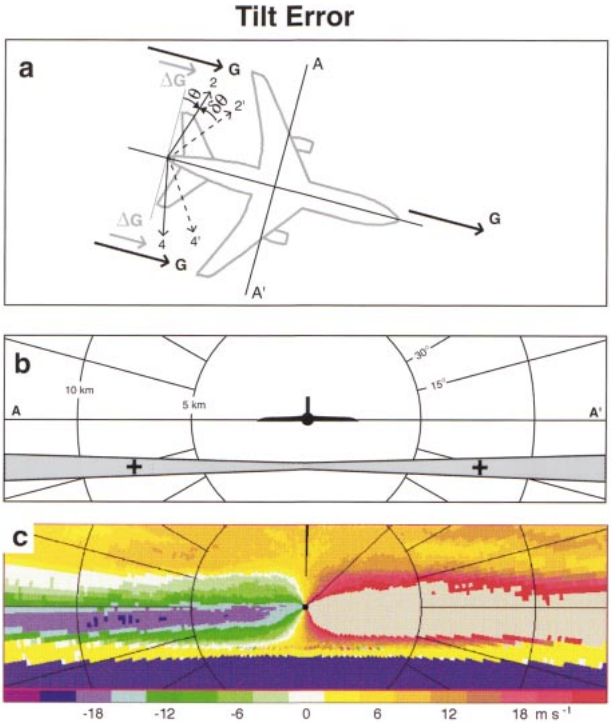

FIG. 3. Same as Fig. 1 but for a negative tilt error.

apparent aircraft motion vector along the apparent track[3] (track 2) in response to a negative $\delta\alpha$ (the arrow for $\delta\alpha$ is pointing toward the direction needs to be corrected and the arrow convention is used for δ quantities in all figures discussed in section 3). The fore (forward looking) radar measures the components of $-\mathbf{G1}$ and $-\mathbf{G2}$ because the component of the earth-relative motion is toward the aircraft. If the **G1** component is added to the fore radar's measured velocity along each beam, the residual velocities on the stationary earth's surface should become 0 m s^{-1}. Adding the **G2** component, the error vector, $\Delta\mathbf{G} = \mathbf{G2} - \mathbf{G1}$, appears as the residual velocity of the earth's surface. In the example illustrated in Fig. 1a, $\Delta\mathbf{G}$ points toward the right side of the aircraft and explains the surface velocity pattern observed in Figs. 1b and 1c by the fore antenna (labeled 2 and 4 in the figure). Consequently, the drift error results in an asymmetric residual surface velocity pattern.

b. The ground speed error (δV_H)

The aircraft ground speed is defined as its speed along the aircraft track (Fig. 2a). Using the same convention illustrated in section 3a, the error vector $\Delta\mathbf{G} = \mathbf{G2} - \mathbf{G1}$, where **G1** is the true ground speed vector and **G2** is the apparent ground speed vector. As a result, a negative ground speed correction (G1 < G2) yields a positive ΔG pointing along the track. Since $\delta V_H = -\Delta G$, the fore radar measures a positive residual velocity while the aft radar (labeled 1 and 3 in Fig. 2a) senses a negative residual velocity. The ground velocities in the fore (aft) radar subtract (add) a larger (smaller) negative aircraft ground speed than its true value. When $\alpha = 0$, a negative ground speed error ($\delta V_H < 0$) yields a positive symmetric velocity residual (ΔG) in all rotation angles for the fore antenna. When $\alpha > 0$ and $\delta V_H < 0$, the right side residual velocities are more positive than the left side residual velocities (Figs. 2b and 2c).

c. The tilt error ($\delta\theta$)

The tilt is the radar-pointing angle from the plane perpendicular to the spin axis to the beam (Fig. 3a), positive (negative) when the antenna is pointing fore (aft). For a waveguide antenna such as the ELDORA and the P3's French antenna, the tilt uncertainty is $\approx \pm 0.05°$ (THL). When ELDORA uses four frequencies, there is an additional 0.05° error due to the difference between the nominal tilt written on the data header and the true tilt. The tilt error may be different for the fore and aft radars when using different antenna and/or different frequencies. Following the same convention, $\Delta\mathbf{G} = \mathbf{G}\,(\sin\theta_2' - \sin\theta_2)$ where θ_2' is the ap-

[3] Apparent is defined as the quantity measured by INS or other onboard instruments that may contain errors. The apparent track, ground speed, . . . , are defined as the variables recorded on the data tape and are subject to correction to yield the true track, ground speed, ...

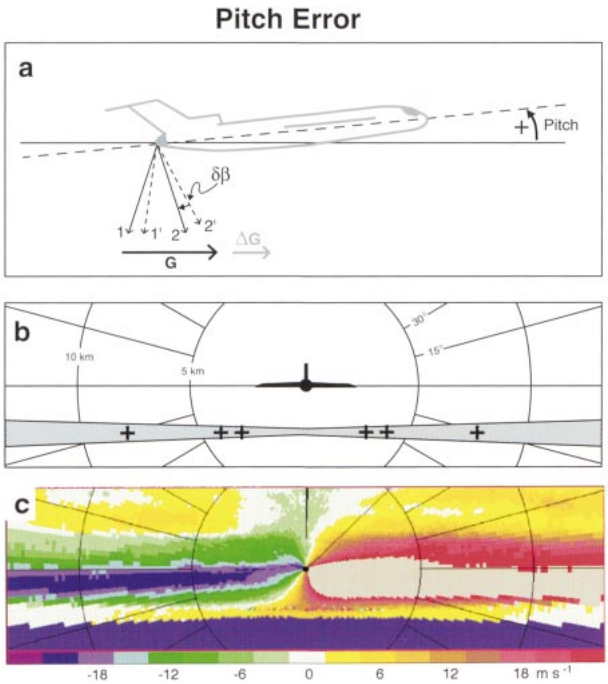

FIG. 4. Same as Fig. 1 but for a negative pitch error. (a) The side view of the error vectors.

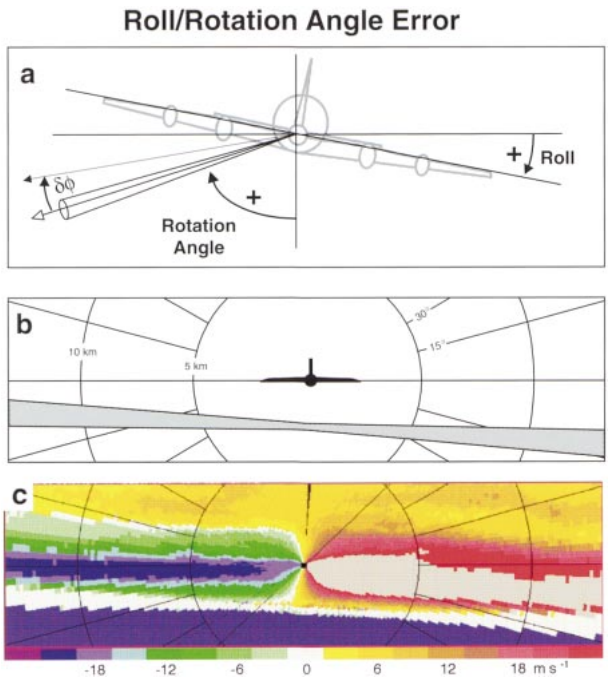

FIG. 5. Same as Fig. 1 but for a negative roll/rotation error. (a) A rear view of the errors.

parent tilt and θ_2 is the true tilt. For $\delta\theta < 0$ ($\theta_2' > \theta_2$) $\Delta\mathbf{G}$ points toward the front of the aircraft and yields a positive surface velocity residual for the fore radar (Figs. 3b and 3c). In this case, the fore radar adds a larger positive component while the aft radar subtracts a smaller positive component to yield the above signature. The velocity signature of a nonzero $\delta\theta$ is symmetric when $\alpha = 0$. When the magnitude of $\delta\theta$ is identical but with opposite sign for the fore and aft radars, the same surface velocity signature can come from a ground speed error. As a result, the tilt error and ground speed error (discussed in section 3b) may be indistinguishable.

d. The pitch error ($\delta\beta$)

Pitch is the angle that the aircraft longitudinal axis makes with the horizontal plane (Fig. 4a). Positive (negative) pitch is defined as nose up (down). The pitch error is defined relative to the radar spin axis. Therefore, the mounting deviation between the radar spin axis and the aircraft longitudinal axis either intentionally or unintentionally will appear as a pitch error in addition to the uncertainty in the INS measured pitch angle. Since the INS measured pitch is rather accurate ($\sim$0.05°), most of the pitch error comes from the mounting error. For example, the NCAR ELDORA antenna was mounted at 1.4° up from the aircraft longitudinal axis to compensate for the natural pitch up of the NCAR Electra in the air. This 1.4° appears as a pitch error. For a negative $\delta\beta$, $\Delta\mathbf{G} = \mathbf{G}(\sin\beta_2' - \sin\beta_2)$ is positive for the fore and aft radars. The velocity amplitude is larger near the nadir as shown in Figs. 4b and 4c.

e. The roll/rotation error ($\delta\phi$)

The roll angle is defined as negative (right wing up) and positive (right wind down) from the horizontal (Fig. 5a). The rotation angle is the spin angle of the radar beam along the longitudinal axis of the aircraft. Zero rotation is defined as pointing toward the nadir (to be consistent with THL). The roll/rotation error tilts the earth surface (not level on radar display) as illustrated in Figs. 5b and 5c, hence, the position of each gate mapping into the earth-relative coordinates is affected.

f. The range delay error (ΔR)

The range delay is the time delay between the instance a pulse is transmitted and the instance the receiver is turned on. A receiver turned on after (before) a pulse is transmitted results in a positive (negative) range delay. This time delay can be converted into distance by multiplying the speed of the electromagnetic wave. The range delay error is characterized by a bulge- or concave-shaped earth surface (not shown) beneath the aircraft. The range delay error only causes errors mapping gates into earth-relative coordinates, but will not affect the removal of aircraft motion from the Doppler velocities.

g. The aircraft altitude error (δH)

The aircraft altitude error is not detectable from the radar display. This error only affects the mapping of the data into earth-relative coordinates.

h. The aircraft vertical velocity error (δW)

The aircraft vertical velocity error produces a velocity signature similar to the pitch error (section 3d). A negative vertical velocity error creates a negative Doppler velocity residual and the largest amplitude is beneath the aircraft (not shown). Since the vertical velocity error is usually less than 0.15 m s^{-1} (THL), the error is often much smaller than other errors after it is projected onto each beam.

4. Effects of these errors/biases on a dual-Doppler analysis

The previous section discusses the important errors that may be encountered when using airborne Doppler radar and the characteristic signatures as they would appear on a radar display. This section illustrates how these errors affect the quality of the dual-Doppler wind analysis and its first-order derivatives. The sensitivity of the dual-Doppler analysis to errors in each individual parameter is presented. The discussion is focused on the effect from five individual parameters (drift, ground speed, tilt, pitch, roll/rotation) that are likely to contain large errors. Flight legs from FASTEX and the verification of the rotation in tornadoes experiment (VORTEX; Rasmussen et al. 1994) are selected to illustrate the individual and combined effects of navigation errors. The VORTEX dataset is the 16 May 1995 Garden City, Kansas, tornado (Wakimoto and Liu 1998; Wakimoto et al. 1998) and the FASTEX dataset is the 12 January 1997 (IOP2) over the northern Atlantic Ocean (Wakimoto and Bosart 2000). The individual effects are investigated by adding a 0.5° error to each angle parameter and 1 m s^{-1} error to the ground speed. Accordingly, five dual-Doppler analyses were performed with an error appearing in only one parameter. Each Doppler analysis was compared to a wind synthesis obtained by implementing all correction factors (the control analysis). A sixth dual-Doppler analysis was performed by including all five errors.

Our study shows that the error in each of these five parameters affects the dual-Doppler radar winds and the first-order derivatives in a somewhat different manner. The sensitivities of the dual-Doppler wind direction, vorticity, and vertical velocity to errors in each individual parameter are presented in Figs. 6, 7, and 8, respectively.

Illustrated with the FASTEX data, major errors in wind direction (Fig. 6) occur along the cold front (~10–20 km left of the flight track). The wind direction is more sensitive to errors either in drift, tilt, or roll/rotation while ground speed and pitch errors have a secondary effect. Owing to the nonlinear effects among all these parameters, the maximum wind direction errors (Fig. 6a) are ~3° along the front to the left of the flight track, which is smaller than that caused by the errors from a single parameter. However, a 5° error occurs to the right of the flight track that exceeds the sum of errors from individual parameters. This illustrates that the total errors are complex and not equal to a simple sum of all errors shown in Figs. 6b–6f. It is noted that the wind direction errors from the drift, ground speed, and pitch biases (Figs. 6b, 6c, and 6d) are symmetric (same sign) across the flight track while the wind direction errors from tilt and rotation/roll biases (Figs. 6e and 6f) are asymmetric (opposite sign) across the track. These characteristics have important implications in identifying error sources discussed in section 6.

The wind speed errors (not shown) are more sensitive to the errors in roll/rotation, pitch, and ground speed. The maximum wind speed errors (~2 m s^{-1}) from all five error sources are larger than those caused by errors in individual parameters.

The errors in vertical vorticity (Fig. 7, illustrated with the FASTEX data) are primarily produced by roll/rotation or pitch errors. Tilt, ground speed, and drift errors have secondary effects. The maximum vorticity error ($\sim -1 \times 10^{-3}$ s^{-1}) in Fig. 7a is larger than the errors from any single source in Figs. 7b–7f. Note that the vorticity is not sensitive to the errors in either drift or ground speed. The latter may be due to the fact that the derivative field is computed locally. The first-order derivatives of the velocity field are relatively unaffected when adjacent grid points are all contaminated by similar errors in wind direction and/or wind speed. Note that the maximum vorticity error pattern occurs within the front and results in an underestimate of the true vorticity in this example.

The vertical velocity error (Fig. 8) is illustrated in a convective situation using the VORTEX data because the amplitude of the vertical velocity is larger than that in the stratiform rain in the FASTEX examples shown earlier. Note that the error is more sensitive to roll/rotation and tilt errors while the pitch error is of secondary importance. Similar to that in the vertical vorticity field, the drift and ground speed errors have almost no effect on the vertical velocity at the 3-km level (integrating upward).

In summary, the dual-Doppler velocities and their derived vorticity and vertical velocity fields are most sensitive to roll/rotation and tilt errors. Pitch errors produce a secondary effect. Errors in all three angles affect the mapping of the Doppler velocity to an earth-relative coordinate system. The mapping error violates the dual-Doppler radar analysis assumption that two velocity components are measured from the same point in space.

For the NCAR ELDORA, the roll/rotation error can be as large as 3° while the pitch error is ~1.4° based on our experience in several field experiments (Table

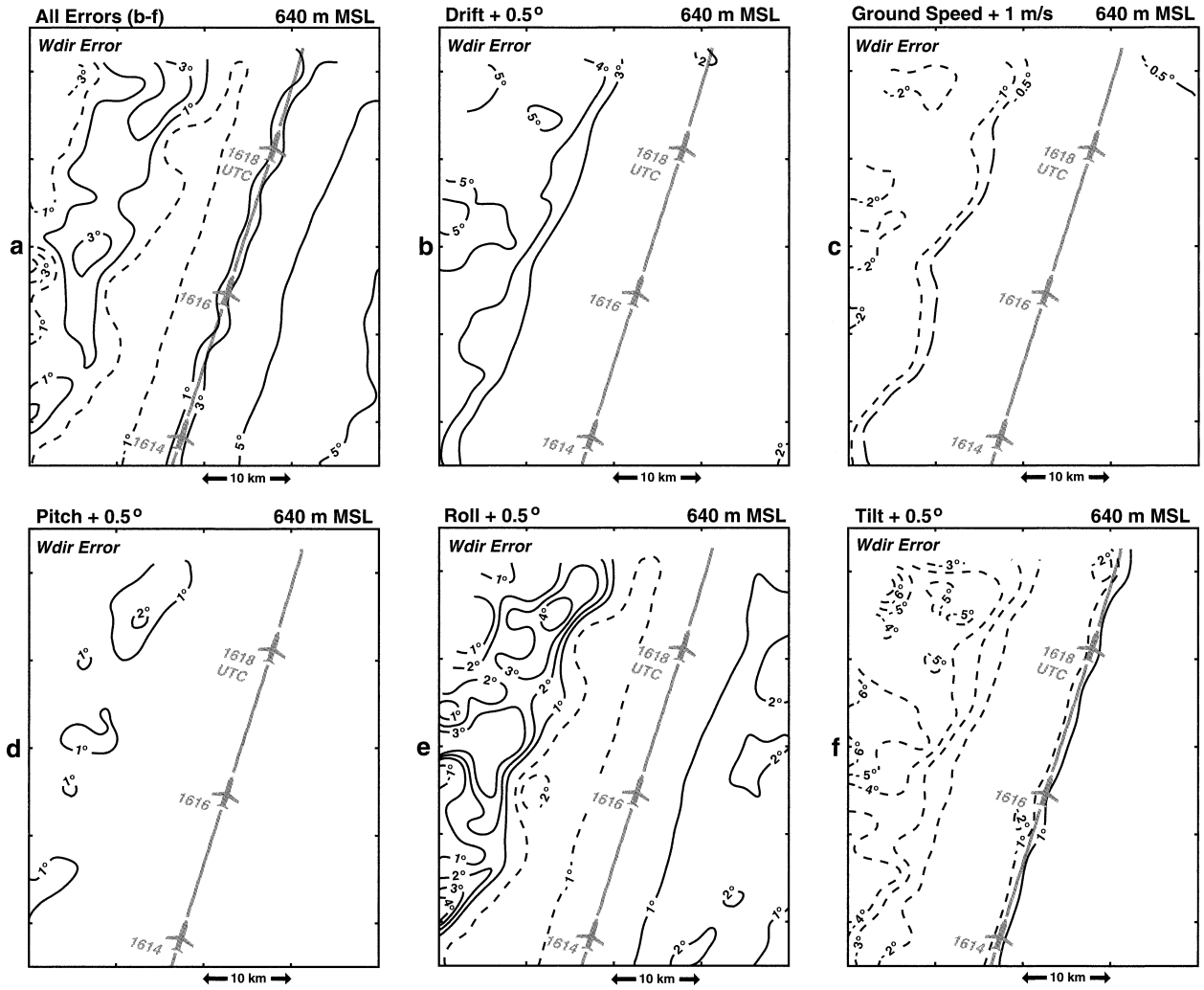

FIG. 6. Error sensitivity in wind directions (°) for the FASTEX cold front case due to (a) all errors, (b) drift error only, (c) ground speed error only, (d) pitch error only, (e) roll/rotation error only, and (f) tilt error only. The aircraft symbols and the thick gray line represent the NCAR Electra flight track. The solid (dashed) lines represent positive (negative) errors in wind direction compared with the control run. All errors in angle parameters are arbitrarily assigned 0.5° while the ground speed error is assigned 1 m s^{-1}.

1). Both of these errors are at least 3 times larger than those errors used for the sensitivity tests examined in this section. Therefore, errors from these two sources cannot be ignored in performing dual-Doppler analysis. Fortunately, the THL and Georgis et al. (2000) methods resolve these two errors quite accurately and leave the major uncertainties in drift, ground speed, and tilt.

5. Development of the Extended THL method

It has been illustrated in THL (summarized in section 2 and the appendix) that drift, ground speed, and tilt cannot be unambiguously determined because there are only two equations relating three unknowns. The accuracy of the electronic steering antenna, such as the French antenna mounted on the NCAR Electra, and NOAA P3, should be within ±0.05° (THL). Therefore, THL assumed the tilt error in the ELDORA antenna during TOGA COARE was negligible so the nonzero residual surface velocities resulted only from drift and ground speed errors. Also, since the ELDORA used only one transmitter in TOGA COARE where the fore and aft radars operated on the same frequencies, tilt errors (if present) had the same magnitude with opposite sign for the fore and aft radars and could be attributed mistakenly as an error in ground speed.

The ELDORA system used its complete two-transmitter configuration during VORTEX-95 (Wakimoto et al. 1996). Because the fore and aft radars transmitted at different frequencies, the tilt errors in the fore and aft radars could be different. In theory, the pointing angles of the waveguide antenna should be accurate within ±0.05°. However, the THL method indicated that errors in tilt were several times larger than the antenna manufacturer's specification.

Since the tilt errors were unknown, the THL proce-

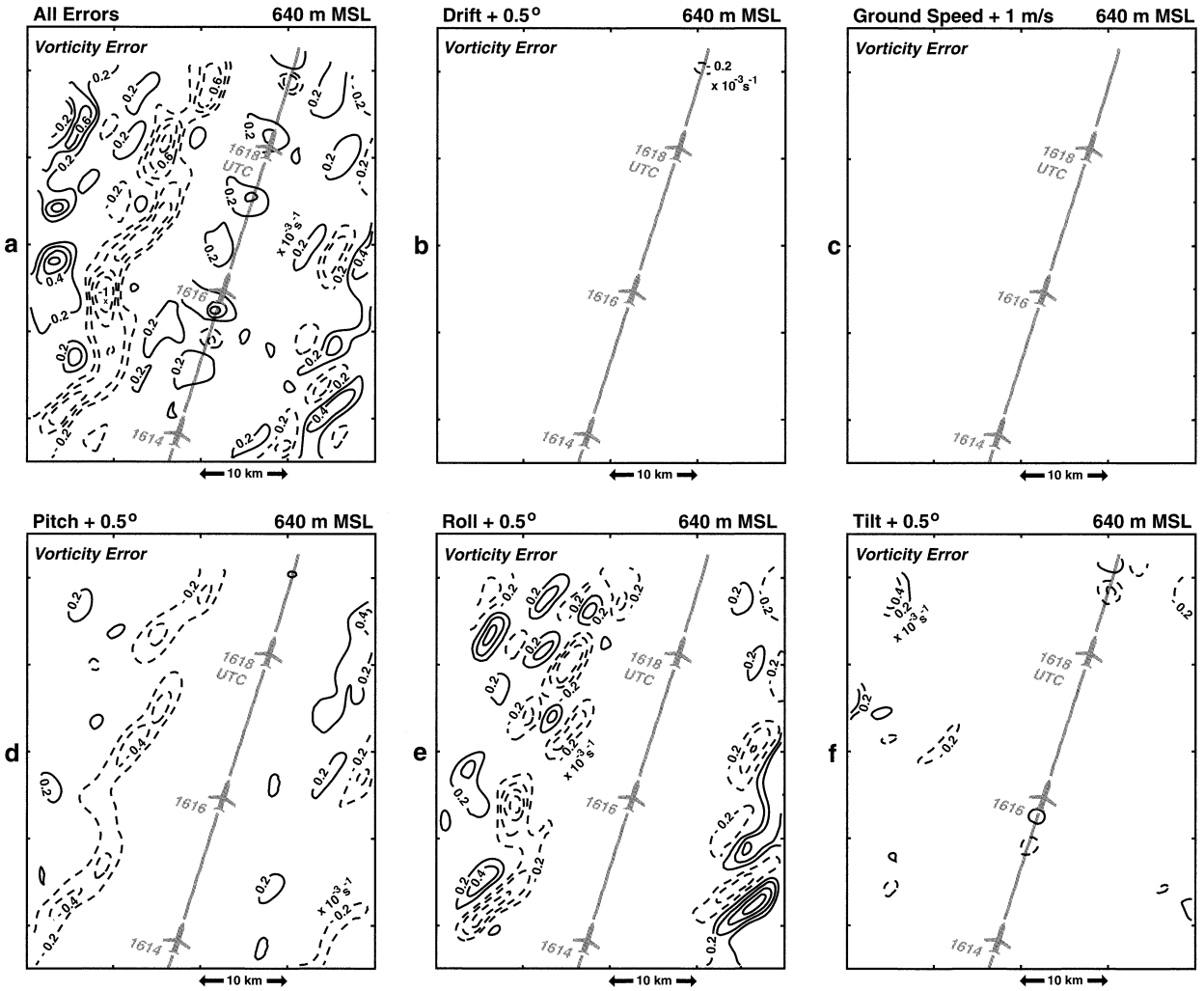

FIG. 7. Same as Fig. 6 except for the error sensitivity in vorticity (in 10^{-3} s^{-1}).

dure was run separately on fore and aft radars assuming no errors for all parameters. The iterative process was terminated when the tilt angle corrections either converged (i.e., stabilized) or were oscillating between two numbers. Note that there may be more than one combination of tilt, drift, and ground speed corrections that can lead to near-zero residual surface velocities. Therefore, the purpose of running the THL method on fore and aft radars separately is to reduce the possible range of tilt corrections. At this point, the ground speed corrections for the fore and aft radars may be different due to the potential uncertainty inherited in running fore and aft radars separately (THL). Once the initial tilt corrections are determined, the fore and aft radar data are combined to determine the ground speed and drift corrections. This procedure produces an improved estimate of tilt, ground speed, and drift corrections (THL). Additional tilt corrections can be made to the fore and/or aft data to force the surface velocity residual to approach 0 m s^{-1}. For the 7 May 1995 flight, the correction factors obtained by the THL method are shown in Table 1. Note that the tilt angle corrections were $-0.2°$ and $0.3°$ for the fore and aft radars.

For a typical flight, the THL procedure is performed on a limited number of the so-called calibration legs requiring the plane to fly a straight flight leg over a flat and stationary surface at a constant midlevel altitude (typically above 3000 m). The corrections obtained from these calibration legs are averaged and applied to the data for the entire flight. Since the accuracy in drift and ground speed may degrade over the duration of the flight due to the Schuler oscillation and/or inertial drift (Masters and Leise 1993), using a single set of correction factors for the entire flight may introduce $\sim$1–2 m s^{-1} and $\sim 1°$ uncertainties in the ground speed and drift corrections. The effect of these errors on the dual-Doppler analysis was discussed in section 4.

Since pitch and aircraft vertical velocity errors are usually determined accurately, the nonzero residual surface velocities in the fore or aft radar result from the

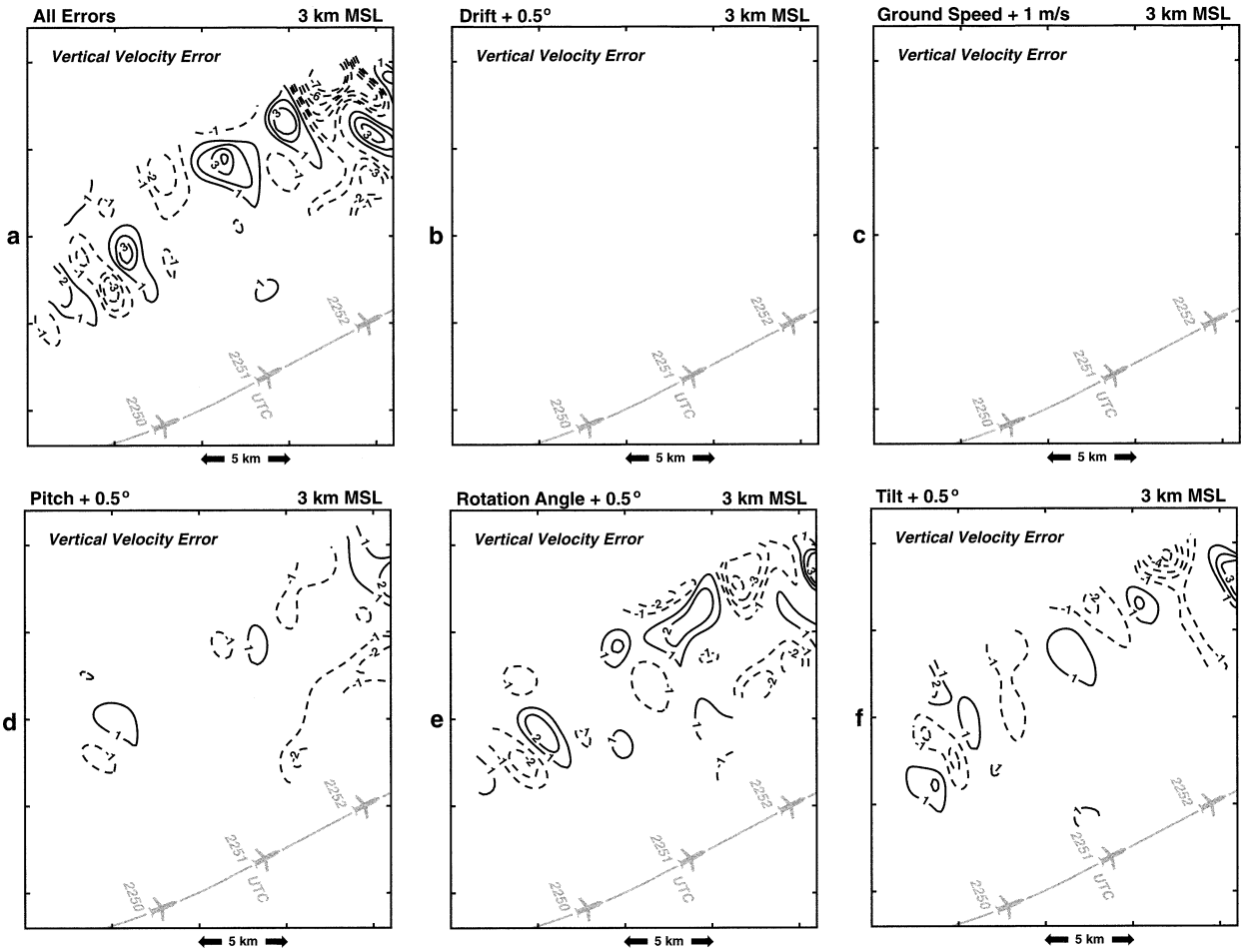

FIG. 8. Same as Fig. 6 except for the error sensitivity in vertical velocity (in m s^{-1}) for a VORTEX supercell case at 3-km above ground level.

errors in tilt, drift, and ground speed. It has been consistently observed that the surface residual velocities have a nonzero bias after applying the THL corrections. This suggests that additional correction factors beyond the standard corrections are required to remove these biases in the surface residual velocities. The ETHL method is presented to identify additional corrections. The ETHL method analyzes the surface residual velocity patterns and the flow chart is illustrated in Figure 9. The mean surface velocity residual on each radar [VL_f (mean velocity of the left fore radar), VR_f (mean velocity of the right fore radar), VL_a (mean velocity of the left aft radar), VR_a (mean velocity of the right aft radar)] can be separated into a symmetric part (A_f and A_a) and an asymmetric part (B_f and B_a). The symbols A and B are defined in the appendix and the subscripts f and a indicate the fore and aft radars. Hence, the symmetric part of the nonzero mean residual velocity, V_{Hf} and V_{Ha}, is computed from A_f and A_a and the asymmetric part of the nonzero mean residual velocity is computed from B_f and B_a (not shown). For the error characteristics illustrated in section 3, the symmetric error is likely due to ground speed error while the asymmetric error is likely due to the drift error. Since there is only one ground speed and drift correction possible for both the fore and aft radars, the ground speed correction is set to the average of V_{Hf} and V_{Ha} while the drift correction is computed from the average of B_f and B_a. These new ground speed and drift corrections are added to the standard THL corrections for this flight to compute the updated Doppler velocities. We use the 7 May 1995 squall

TABLE 1. The correction factors for the 7 May 1995 calibration leg (1950–1957 UTC) using the THL method.

	Fore	Aft
Drift	−0.1°	−0.1°
Pitch	−1.4°	−1.4°
Ground speed	−0.8 m s^{-1}	−0.8 m s^{-1}
Aircraft altitude	−0.03 km	−0.03 km
Range delay	0.17 km	0.16 km
Roll/rotation	2.7°	−1.0°
Tilt	−0.2°	0.3°

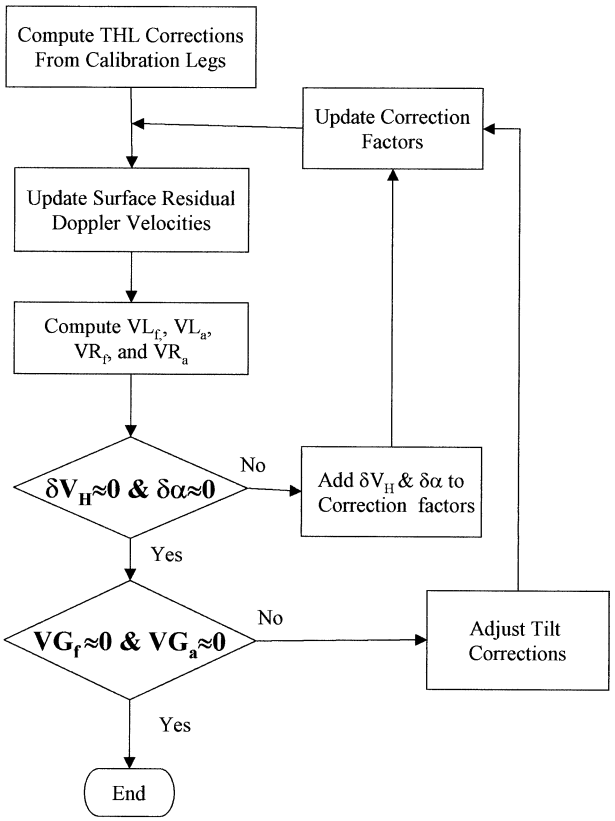

FIG. 9. The flowchart of the ETHL method.

line data at 2208 UTC as an example to illustrate the iterative process, beginning with the set of correction factors obtained from the calibration leg (Table 1). As illustrated in Table 2, the ground speed and drift errors are reduced significantly after the first iteration and both of these corrections were near zero after three iterations. However, the ground speed corrections for the fore and aft radars (V_{Hf} and V_{Ha}) after three iterations were nearly equal in magnitude but with opposite signs. This signature indicates that the mean residual velocity for each individual antenna cannot be further reduced by simply adjusting the ground speed correction. Accordingly, this error is likely caused by a tilt error, equal in magnitude and sign, for both the fore and aft radars (discussed in section 3). Subtracting 0.1° from the tilt corrections (in Table 1) from both the fore and aft radars (the fourth iteration), the mean residual velocities are near zero for both radars. This approach has been applied to seven different legs in the 7 May 1995 squall line case and the tilt angle corrections (not shown) are consistent with the results shown in Table 2.

6. Determine corrections over a moving earth surface

The THL approach and the ETHL method discussed in section 5 are only valid when the earth surface is flat

TABLE 2. The iterative process of the ETHL method on 2028 UTC 7 May 1995 leg. Each row represents a different iteration. The first three iterations used tilt corrections of −0.2° (0.3°) for the fore and aft radar. The fourth iteration used tilt corrections of −0.3° (0.2°) for the fore and aft radar. The V_{Hf} and V_{Ha} are computed from A_f and A_a using (3) assuming $\alpha = 0°$ and $\theta = 18°$. The δV_G is the average of V_{Hf} and V_{Ha}. The $\delta\alpha$ is computed from the average of β_f and B_a assuming $\alpha = 0°$, $\theta = 18°$, and $V_G = 120$ m s^{-1}. All units are in m s^{-1} except for $\delta\alpha$ (in °). See text for the definition of symbols.

Iteration	1	2	3	4
VL_f	−0.28	0.08	0.13	−0.05
VR_f	−0.16	0.13	0.18	−0.01
VL_a	0.45	0.29	0.24	0.04
VR_a	0.6	0.15	0.1	−0.09
A_f	−0.22	0.105	0.155	−0.03
A_a	0.525	0.22	0.17	−0.025
B_f	−0.06	−0.025	−0.025	−0.02
B_a	−0.075	0.07	0.07	0.065
V_{Hf}	0.71	−0.34	−0.50	0.10
V_{Ha}	1.70	0.71	0.55	−0.08
$\delta\alpha$	−0.03	0.01	0.01	0.01
δV_H	1.20	0.19	0.02	0.01

and stationary. When observing weather systems over water, the motion in the surface adds another degree of freedom to the problem because the residual surface velocity cannot be assumed zero. An additional independent measurement, such as the flight-level wind, is required to anchor the solution in drift, tilt, and ground speed corrections. The new method, the BLW method, is based on three constraints. First, the in situ winds are statistically consistent with the dual-Doppler winds near the aircraft at the flight level. Note that the Global Positioning System corrected in situ winds for the INS Schuler oscillation and inertial drift should be used in this comparison. Second, the dual-Doppler winds across the track are continuous (i.e., the wind direction and wind speed are statistically consistent across the track). Third, the residual surface velocities in the left (right) fore radar should have approximately the same magnitude but opposite sign as the right (left) aft radar Doppler velocities owing to a moving surface.[4] The BLW method can be applied when dual-Doppler winds are reliably retrieved near the aircraft for a long period of time (e.g., flying in extensive precipitation or in regions with clear air return).

The BLW method is an iterative process that follows four basic steps (flowchart is illustrated in Fig. 10). First, select a straight flight leg at a near-constant altitude, preferably in an extensive precipitation region with little horizontal shear across the aircraft (i.e., the track should not coincide with a frontal zone or a gust front). Second, create a dual-Doppler wind synthesis at flight level. The origin of the analysis should be placed at the halfway point of the track and only the dual-Doppler winds with-

[4] This tractable methodology to compute navigation corrections for moving surface echoes benefits from early discussions with P. Hildebrand (1997, personal communication).

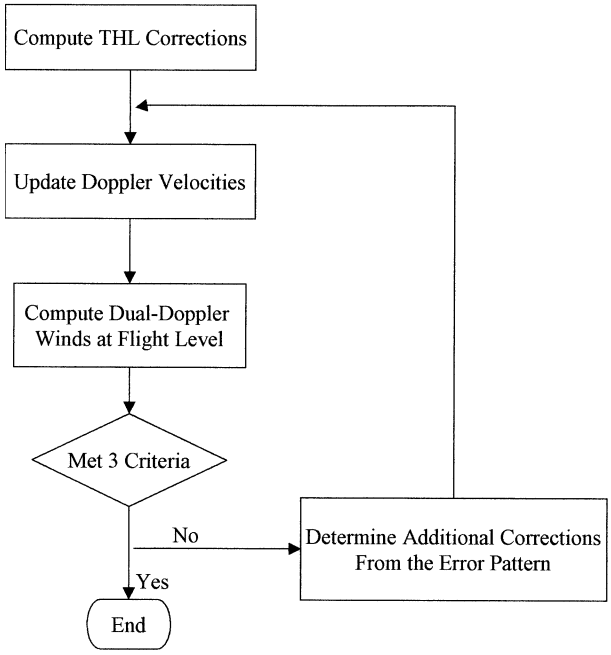

FIG. 10. The flowchart of the BLW method.

in 1 km on either side of the aircraft should be selected for the comparison to minimize the effect of horizontal shear. It is preferable to choose one of the coordinate axes parallel to the mean aircraft track so that winds can be separated into along-track (v) and cross-track (u) components. The dual-Doppler analysis of a relatively long leg should be performed in segments to alleviate the mapping errors due to the earth curvature in a Cartesian grid. Third, map the in situ winds to the nearest dual-Doppler grid points. The in situ winds are usually sampled in 1-s intervals (~120-m resolution) and the grid spacing for the dual-Doppler analysis is normally ~500 m for the NCAR ELDORA and ~1500 m for the NOAA P3. Therefore, the in situ winds should be filtered to match the spatial scale resolved by the dual-Doppler winds. Fourth, statistically compare the in situ winds and dual-Doppler winds using the mean and standard deviation of the wind direction and wind speed over the chosen time period. In addition, root-mean-square (rms) errors should be computed. If a discrepancy exists, adjust drift, ground speed, and tilt then restart the process from step 2 until all three criteria are satisfied.

Two important rules are used as guidelines to identify the additional adjustments of the parameters in the fourth step. Ground speed and tilt corrections affect the along-track component of the dual-Doppler winds while the drift correction affects the cross-track component of the dual-Doppler winds. For example, a positive ground speed correction increases the mean along-track wind speed and a positive drift correction shifts the mean wind direction clockwise. Therefore, the drift, ground speed, and tilt corrections can be estimated and the Doppler velocities are adjusted in order to satisfy the three criteria stated in this section.

7. Results of the BLW method

The BLW method is illustrated using case studies in 7 May 1995 during VORTEX 95 (over land) and 12 January 1997 during FASTEX (over ocean). The drift, tilt, and ground speed corrections were obtained using the BLW method (referred to as the ''BLW corrections''). The BLW corrections for both cases are listed in Table 3. The standard 'THL corrections' for the VORTEX 95 case are also listed in Table 3. The THL corrections for the VORTEX case are obtained assuming $-0.2°$ (fore) and $0.3°$ (aft) tilt corrections. Note that the tilt angle corrections obtained between the THL and the BLW methods differ by $0.1°$. As illustrated in section 5, this $0.1°$ can be accounted for by the ETHL method. Hence, the tilt corrections obtained from the BLW method and the ETHL method are consistent. However, there is a noticeable shift of $0.3°$ in tilt corrections between the VORTEX and FASTEX data using the BLW method (Table 3). It is not clear why this is the case and some possible reasons are discussed in the next section. Two dual-Doppler wind syntheses were performed with the BLW corrections and with no corrections. The statistical

TABLE 3. The correction factors obtained from the THL method and the BLW method for the 0057 UTC 8 May 1995 VORTEX flight leg and the 1600 UTC 12 Jan 1997 FASTEX flight leg.

	VORTEX (0057 UTC 8 May 1995)		FASTEX (1600 UTC 12 Jan 1997)
Corrections	THL corrections	BLW corrections	BLW corrections
Range delay fore	175.0 m	175.0 m	264.0 m
Range delay aft	170.0 m	170.0 m	257.0 m
Aircraft altitude	55.0 m	55.0 m	68.0 m
Ground speed	0.8 m s^{-1}	1.0 m s^{-1}	1.0 m s^{-1}
Drift	$-0.2°$	$-0.1°$	$-0.3°$
Pitch	$-1.5°$	$-1.4°$	$-1.4°$
Roll/rotation fore	$2.7°$	$2.7°$	$2.4°$
Roll/rotation aft	$-1.1°$	$-1.1°$	$2.8°$
Tilt fore	$-0.2°$	$-0.3°$	$-0.0°$
Tilt aft	$0.3°$	$0.2°$	$0.5°$

TABLE 4. The statistical analyses among the in situ winds, dual-Doppler winds with no corrections, and dual-Doppler winds with BLW corrections for the FASTEX 1710 UTC 12 Jan 1997 leg.

FASTEX (12 Jan 1997 1710 UTC)			
Average	In situ	Dual-Doppler (no correction)	Dual-Doppler (with BLW correction)
Wind speed	34.84 m s^{-1}	34.52 m s^{-1}	34.82 m s^{-1}
Wind direction	177.2°	175.0°	176.7°
U-component	−1.69 m s^{-1}	−3.01 m s^{-1}	−1.99 m s^{-1}
V-component	34.80 m s^{-1}	34.39 m s^{-1}	34.77 m s^{-1}
U-rms		0.83 m s^{-1}	0.64 m s^{-1}
V-rms		0.44 m s^{-1}	0.36 m s^{-1}
U correlation coef		−0.12	0.21
V correlation coef		0.89	0.91
U intersection		−3.16	−1.81
U slope		−0.09	0.105
V intersection		−1.25	1.69
V slope		1.02	0.95

analysis between these two Doppler wind fields and the in situ winds is shown in Table 4 for FASTEX and Table 5 for VORTEX 95 cases. Also shown in Table 5 is the statistical analysis between the dual-Doppler wind synthesis using the THL corrections and the in situ winds.

In general, the dual-Doppler winds with BLW corrections are statistically closer to the in situ winds than the dual-Doppler winds without any corrections. Although the improvement in the mean wind direction and wind speed by applying the BLW corrections over the no correction cases appears to be small, the rms errors with the BLW corrections are reduced by ~30% and the correlation coefficient increased significantly in both cases. Figures 11 and 12 shows the scatterplots of the uncorrected (top panels) and corrected (lower panels) u and v component between the corrected dual-Doppler wind and the in situ wind in VORTEX and FASTEX. The maximum rms errors are ~0.6 m s^{-1} that are significantly better than those dual-Doppler wind synthesis shown in Marks et al. (1992)[5] and Atkins et al. (1998). This improvement can also be inferred from the slope and intersection of the linear fit shown in Tables 4 and 5 where the corrected data has a slope closer to 1 (a perfect fit) than that of the uncorrected dataset. The correlation coefficient is low in the u component scatterplot of the FASTEX case (lower-left panel in Fig. 12), owing to the distribution of the data over a small velocity range (~2 m s^{-1}). Nevertheless, the u components deduced from the BLW corrected data are statistically superior to the uncorrected data.

The dual-Doppler winds, isogon, and vorticity analysis for the FASTEX IOP2 cold front case is illustrated in Fig. 13. The upper panels are the analyses with the BLW corrections while the lower panels are the analyses without corrections. The NCAR Electra was flying from

[5] Marks et al. (1992) study involved Doppler radar data and flight-level winds from two NOAA P3s flying at different altitudes that contained more uncertainties than the data obtained from a single plane. Therefore, the standard deviation between the dual-Doppler winds and the flight-level winds on their study should be higher compared with the results in this study.

TABLE 5. Same as Table 6 but for the VORTEX 0057 UTC 8 May 1995 leg. The statistics of the dual-Doppler winds with THL corrections are also shown.

VORTEX 95 (8 May 1995 0057 UTC)				
		Dual-Doppler wind		
Average	In situ	No correction	BLW correction	THL correction
Wind speed	35.37 m s	36.31 m s^{-1}	34.96 m s^{-1}	34.78 m s^{-1}
Wind direction	214.2°	214.4°	214.2°	213.6 m s^{-1}
U-component	19.91 m s^{-1}	20.54 m s^{-1}	19.64 m s^{-1}	19.24 m s^{-1}
V-component	29.24 m s^{-1}	29.94 m s^{-1}	28.92 m s^{-1}	28.97 m s^{-1}
U-rms		0.71 m s^{-1}	0.53 m s^{-1}	0.54 m s^{-1}
V-rms		1.24 m s^{-1}	0.56 m s^{-1}	0.48 m s^{-1}
U correlation coef		0.92	0.95	0.95
V correlation coef		0.74	0.95	0.96
U intersection		0.54	1.36	1.18
U slope		0.76	0.92	0.91
V intersection		9.24	5.08	4.42
V slope		0.71	0.82	0.84

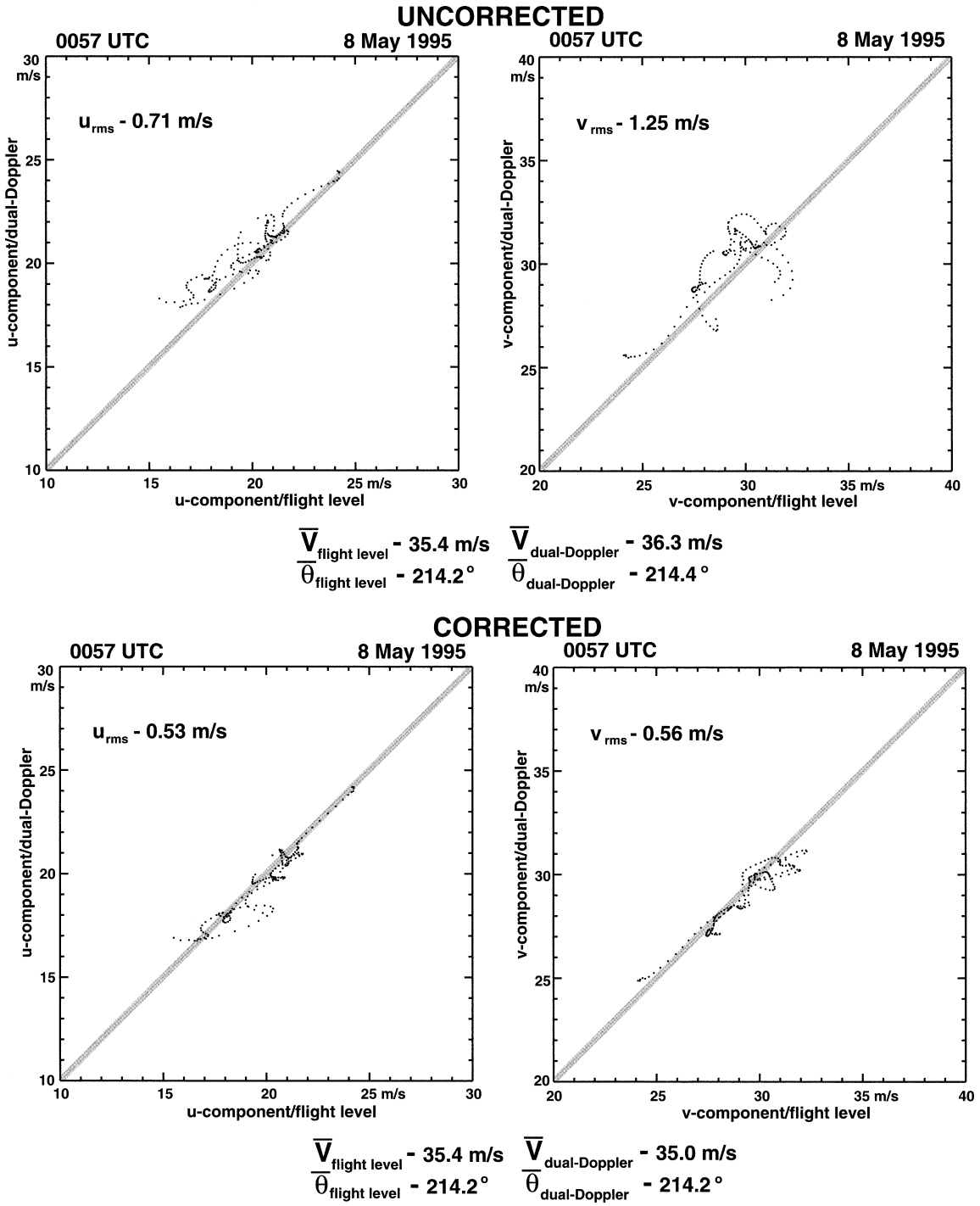

FIG. 11. The scatterplot of the u (cross track) and v (along track) components between the horizontal in situ winds and the dual-Doppler winds (top) without corrections and (bottom) with the BLW corrections for the 0057 UTC 8 May 1995 flight leg. The thick gray line represents the perfect match between the dual-Doppler and the in situ wind components.

SSW to NNE along the east side of a cold front (marked by the wind shift and high vorticity). The wind fields (vectors) in the upper panels clearly resolve a sharper wind shift along the cold front than those shown in the lower panels. The sharp gradient is also illustrated in the isogon field where a stronger gradient of wind direction is resolved in the corrected data. The maximum vorticity in the frontal zone exceeded 6×10^{-3} s^{-1}. Surprisingly, the uncorrected data also resolves a similar pattern and magnitude of vorticity near the frontal zone

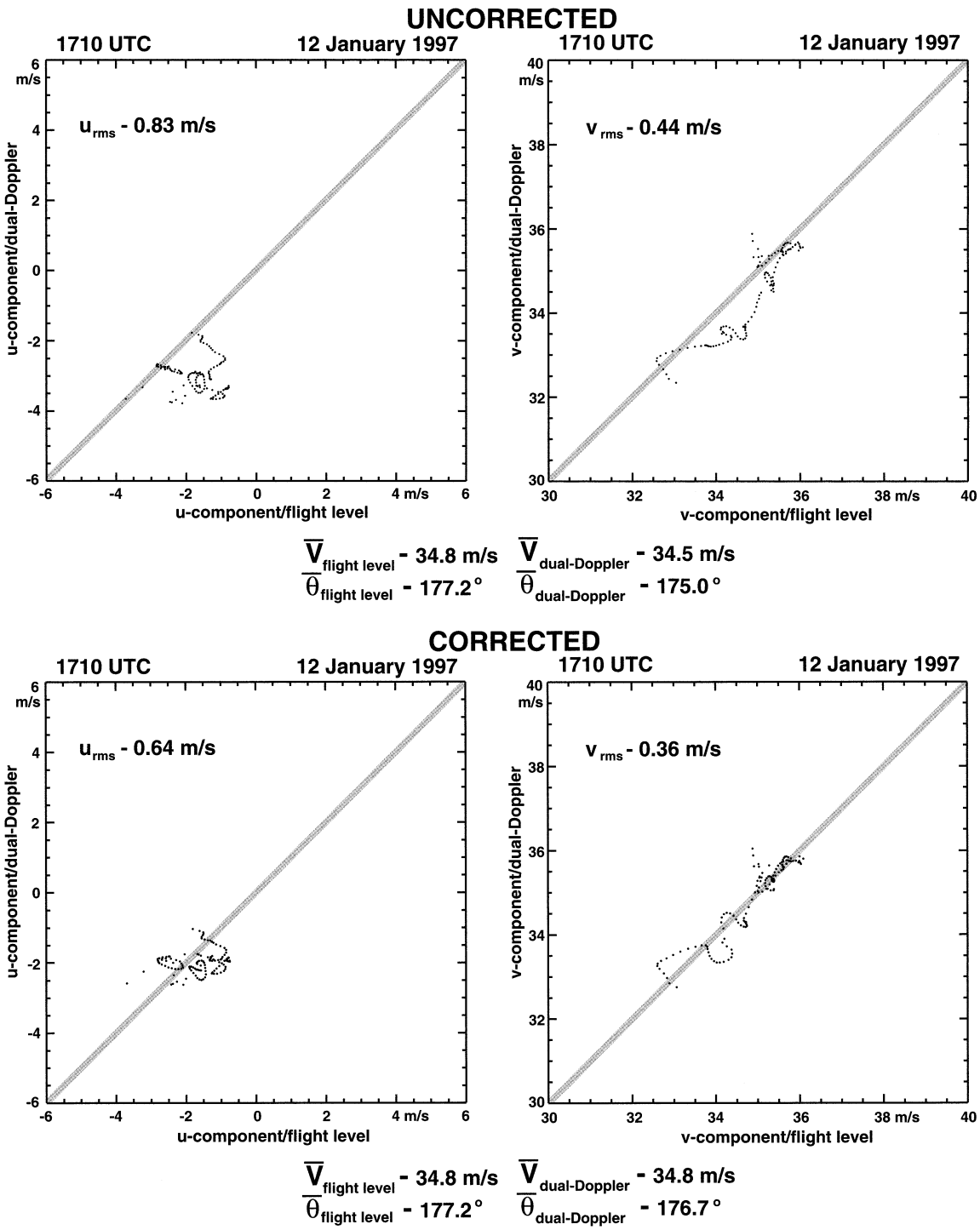

FIG. 12. Same as Fig. 11 but for 1700 UTC 12 Jan 1997.

even though the wind field contains errors. The uncorrected data, however, also produces spurious vorticity near the flight track and on the right of the flight track. This example illustrates the importance of applying the proper navigation and radar-pointing angle corrections before performing dual-Doppler analysis.

8. Discussion

The tilt of an electronically steered waveguide antenna, in theory, should not contain significant errors other than the 0.05° uncertainties (THL). The analyses presented in this paper indicate a much larger error (up

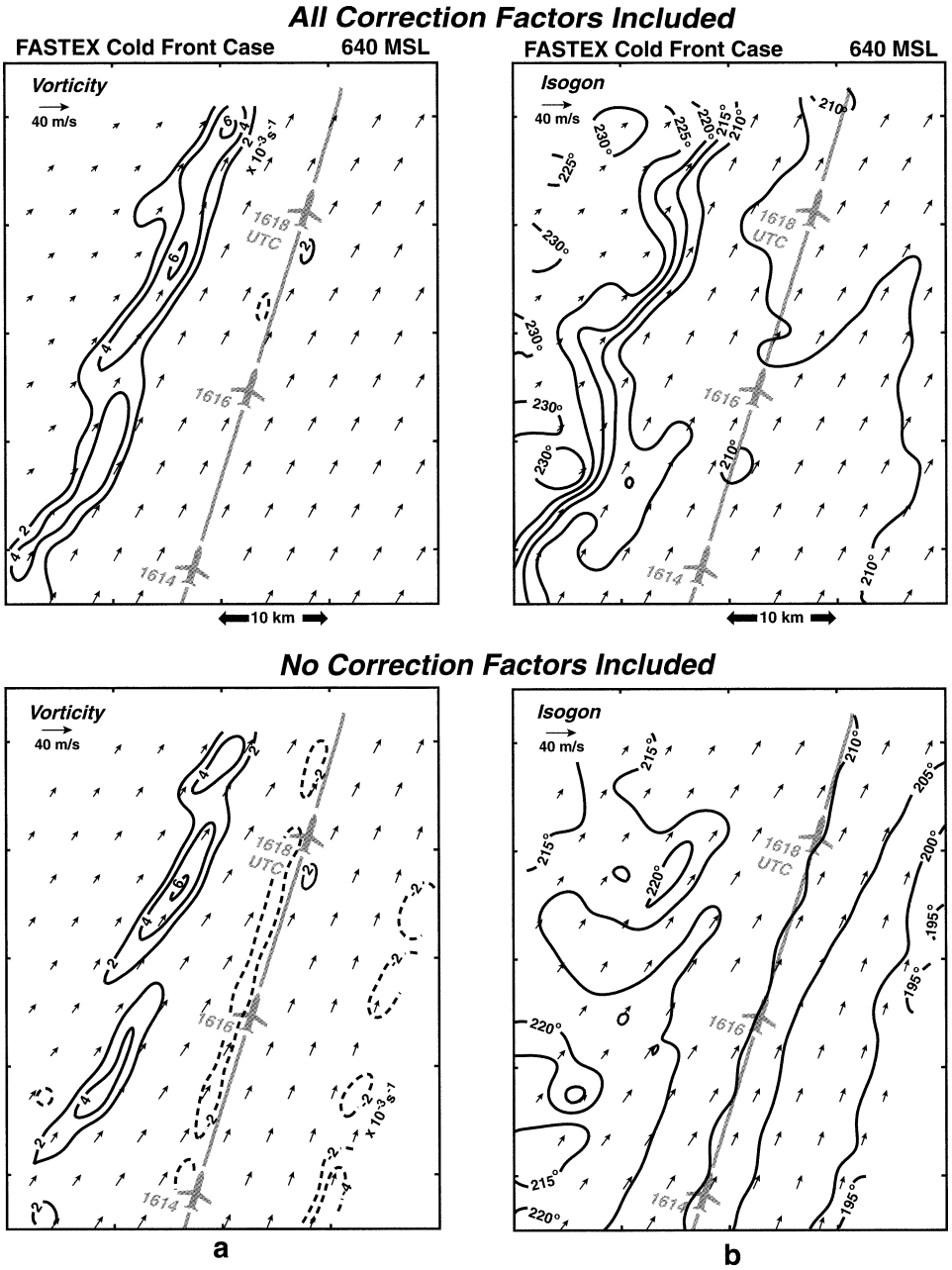

FIG. 13. The comparison of dual-Doppler radar winds (vectors), vorticity, and isogon between (top) the BLW corrected data and (bottom) the uncorrected data at 1700 UTC 12 Jan 1997. The gray line indicates the flight track of the NCAR Electra. (left) Solid (dashed) lines represent positive (negative) vorticity.

to 0.5°) in the tilt for the NCAR ELDORA antenna. ELDORA engineers have verified via careful measurement that the ELDORA fore and aft antenna are parallel to each other and the spin axis of the rotordome is aligned with the fuselage. Hence, the tilt errors identified in this study for the ELDORA antenna cannot be attributed to the mounting error. It is possible that the manufacturer specification of the beam-pointing angles at different frequencies were incorrect. Since the radar frequencies were nearly identical for the VORTEX and FASTEX, it is not clear why there was a shift of ~0.3° in the tilt corrections between these two field experiments.[6]

[6] P. Hildebrand (2001, personal communication) pointed out that the NCAR ELDORA used primarily three frequencies during FASTEX, compared with four frequencies used during VORTEX, in order to increase the sensitivity of the returns over the ocean. Hence, the pointing angle should be different between these two experiments. In practice, the ELDORA pointing angles recorded on the tape were

TABLE 6. Comparison of the theoretical uncertainties of individual parameters documented in THL and their corresponding values found in the 0057 UTC 8 May 1995 flight leg.

	THL	08 May 1995
A	0.1 m s^{-1}	0.3 m s^{-1}
B_1	0.1 m s^{-1}	0.36 m s^{-1}
B_2	0.1 m s^{-1}	0.36 m s^{-1}
C	10 m	8 m
D_1	10 m	6 m
D_2	10 m	5 m
ΔR	±20 m	±15 m
$\delta\alpha$	±0.05°	±0.17°
$\delta\beta$	±0.05°	±0.16°
$\delta\phi$	±0.15°	±0.18°
$\delta\theta$	±0.05°	±0.13°
δV_H	±0.3 m s^{-1}	±0.98 m s^{-1}
δH	±10 m	±4 m

The individual correction factor deduced from the THL method varied from sweep to sweep. The final correction factors were the mean value for as many sweeps available in the calibration leg (usually between 50 and 100 sweeps). The statistical approach implemented in the BLW method followed a similar procedure. Therefore, the accuracy of the corrections obtained in the THL method depends on the uncertainties (standard deviation) in these individual parameters among all sweeps in the analysis. Table 6 compares the nominal uncertainties of the coefficients and in each parameter documented in THL and the standard deviation of these parameters in the 7 May 1995 VORTEX 95 case. Except for similar magnitude in the roll/rotation, aircraft altitude, and the range delay, the standard deviations in all other corrections are about 3 times higher than those documented in THL. As a result, the uncertainty in tilt correction is ~0.13°, suggesting that the 0.1° difference in tilt corrections between the THL and the BLW methods in the 7 May 1995 case may be statistically insignificant. However, this argument cannot explain why there is a ~0.3° shift in tilt corrections between the VORTEX and FASTEX data using the BLW method.

9. Summary and conclusions

Two new procedures were presented in this study to further improve the accuracy of the airborne Doppler radar data beyond the pioneering method presented in THL to systematically identify the errors/biases in the INS-derived parameters and radar-pointing angles. It was shown that the THL method could accurately identify the errors in pitch, aircraft vertical velocity, range delay, aircraft altitude, and roll/rotation, but left major uncertainties in drift, ground speed, and tilt owing to the nature of an underdetermined problem. In addition, the THL method is not accurate when applied over a moving earth surface. This paper addresses these uncertainties.

Errors in each of the eight parameters in the INS navigation and radar-pointing angle errors were shown to affect both the dual-Doppler winds and their first-order derivative quantities in different manners. For instance, drift or ground speed errors only affect the accuracy of the dual-Doppler wind vectors while errors in roll/rotation, tilt, and pitch affect both the dual-Doppler winds and their derived vorticity and vertical velocity fields.

It was found in several experiments that the drift and ground speed errors might change with time due to the INS drift and/or Schuler oscillation. Therefore, an extra 1° in drift correction and 1 m s^{-1} correction in ground speed may be required in addition to those obtained from the calibration leg. The ETHL method was proposed to fine-tune the drift, ground velocity, and tilt corrections on flight legs other than the calibration leg. It was shown that additional corrections on drift, tilt, and ground speed can be identified by analyzing the symmetric and asymmetric surface residual velocity patterns on each flight leg using a set of correction factors computed from the calibration leg. As a result, the overall quality of the dual-Doppler wind analyses was improved by implementing the ETHL method.

The BLW method was proposed to identify the drift, ground speed, and tilt errors over a moving earth surface to complement the ETHL method. The BLW method can be applied when reliable dual-Doppler winds at the flight level can be retrieved on both sides of the aircraft. The BLW method forces the dual-Doppler radar winds at the flight level near the aircraft to statistically match the in situ winds over a flight leg by adjusting all eight parameters. In addition, the BLW method requires the dual-Doppler winds across the flight track to be continuous and the surface residual velocities to be consistent with the surface motion vector. In the FASTEX example, the BLW corrected wind fields clearly show the sharp transition of winds across the cold front while the uncorrected dual-Doppler winds show a much smoother transition. The dual-Doppler winds using the BLW corrections are clearly superior to the dual-Doppler winds without any corrections. Consistent results obtained between the ETHL method and the BLW method using VORTEX data confirm that the BLW method can also be used over land.

This paper reinforces the fact that identifying correction factors for airborne Doppler radar is a nontrivial problem and no single method will work in all situations. The ETHL method and the BLW method proposed in this paper, however, appear to produce datasets containing the least amount of error. These two methods are subject to their own limitations. The ETHL method can only be applied to a flat and stationary earth surface.

the angles of the middle frequency and the angle was the same whether using three or four frequencies. With a 10 MHz frequency separation for the ELDORA, the pointing angle error between using three and four frequencies should be 0.05°. Therefore, the error cannot explain the 0.3° to 0.5° errors found in this study.

The BLW method can be applied to all surface conditions but can only be exercised when the aircraft flies in extensive precipitation or is able to retrieve velocities in the clear air. Nevertheless, this paper presents new approaches to extend the current capability in refining navigation and radar-pointing angle uncertainties, especially over a moving earth surface. Contrary to the previous belief that the tilt angles are nearly perfect (THL), this paper illustrates that the uncertainty in tilt can be as large as 0.5°. This error, if not corrected, will seriously degrade the dual-Doppler winds. Users of airborne Doppler radar data are strongly encouraged to take extra steps to ensure the quality of the dual-Doppler winds and their derived quantities.

Acknowledgments. The authors thank Ms. Susan Stringer for programming support. The careful review of this manuscript and insightful discussions with Dr. Peter Hildebrand, Mr. Peter Dodge, Dr. Tammy Weckwerth, Mr. Scott Ellis, and Mr. Craig Walther are greatly appreciated. This research is partially sponsored by the National Science Foundation under Grants ATM-9801720 and 0121048.

APPENDIX

Summary of Key Equations in THL

THL derived two sets of equations [(10) and (18) in THL] that govern the error characteristics of the eight parameters as a function of the rotation, ϕ:

$$\begin{aligned}\delta V_G &= V_G - V_{Ge} \\ &= A + B_1 \sin\phi + B_2 \cos\phi \qquad \text{(A1)}\\ \cos^2\phi\,\delta R_G &= \cos^2\phi(R_G - R_{Ge} + \Delta R) \\ &= C + D_1 \sin\phi + D_2 \cos\phi \\ &\quad + E \cos 2\phi. \qquad \text{(A2)}\end{aligned}$$

The symbols V_G (V_{Ge}) and R_G (R_{Ge}) are, respectively, the measured (estimated) ground velocity and distance between the radar and ground for each beam. Recall that the zero rotation is defined as pointing toward the nadir in THL. The corresponding coefficients *A–E* from the Fourier analysis are expressed as follows (please see text for the meaning of these symbols):

$$\begin{aligned}A &= -V_H \cos\alpha \cos\theta\delta\theta \\ &\quad + \sin\theta(V_H \sin\alpha\delta\alpha - \cos\alpha\delta V_H) \qquad \text{(A3)}\\ B_1 &= -V_H \sin\alpha \sin\theta\delta\theta \\ &\quad + \cos\theta(V_H \cos\alpha\delta\alpha + \sin\alpha\delta V_H) \qquad \text{(A4)}\\ B_2 &= \cos\theta\delta W - V_H \cos\alpha \cos\theta\delta\beta \qquad \text{(A5)}\\ C &= -\frac{\Delta R}{2} + \frac{H \tan\theta}{\cos\theta}\delta\beta \qquad \text{(A6)}\\ D_1 &= \frac{H\delta\phi}{\cos\theta} \qquad \text{(A7)}\\ D_2 &= \frac{\delta H + H \tan\theta\delta\theta}{\cos\theta} \qquad \text{(A8)}\\ E &= -\frac{\Delta R}{2}. \qquad \text{(A9)}\end{aligned}$$

The above equations have been simplified by assuming small α and β plus $W \ll V_H$. All delta (δ) quantities are defined as the true value minus the measured value. Therefore, all correction factors obtained in this procedure should be added to their corresponding measured value to yield the estimated true value. A total of seven independent equations govern the eight parameters. These coefficients can be obtained via a least squares fit of the surface velocity residual and the distance residual on all available rotation angles of a single sweep. Please refer to THL for details.

REFERENCES

Atkins, N. T., R. M. Wakimoto, and C. L. Ziegler, 1998: Observations of the finescale structure of a dryline during VORTEX 95. *Mon. Wea. Rev.,* **126,** 525–550.

Chong, M., and O. Bousquet, 1999: A mesovortex within a near-equatorial mesoscale convective system during TOGA COARE. *Mon. Wea. Rev.,* **127,** 1145–1156.

Durden, S. L., Z. S. Haddad, and T. P. Bui, 1999: Correction of Doppler radar data for aircraft motion using surface measurements and recursive least squares estimation. *J. Atmos. Oceanic Technol.,* **16,** 2026–2029.

Georgis, J. F., F. Roux, and P. H. Hildebrand, 2000: Observation of precipitating systems over complex orography with meteorological Doppler radars: A feasibility study. *Meteor. Atmos. Phys.,* **72,** 185–202.

Joly, A., and Coauthors, 1997: The Fronts and Atlantic Storm-Track Experiment (FASTEX): Scientific objectives and experimental design. *Bull. Amer. Meteor. Soc.,* **78,** 1917–1940.

Jorgensen, D. P., M. A. LeMone, and S. B. Trier, 1997: Structure and evolution of the 22 February 1993 TOGA COARE squall line: Aircraft observations of precipitation, circulation, and surface energy fluxes. *J. Atmos. Sci.,* **54,** 1961–1985.

Lee, W.-C., P. Dodge, F. D. Marks, and P. H. Hildebrand, 1994: Mapping of airborne Doppler radar data. *J. Atmos. Oceanic Technol.,* **11,** 572–578.

Marks, F. D., Jr., R. A. Houze Jr., and J. F. Gamache, 1992: Dual-aircraft investigation of the inner core of Hurricane Norbert. Part I: Kinematic structure. *J. Atmos. Sci.,* **49,** 919–942.

Masters, J. M., and J. A. Leise, 1993: Correction of inertial navigation with Loran C on NOAA's P-3 aircraft. *J. Atmos. Oceanic Technol.,* **10,** 145–154.

Rasmussen, E. N., J. M. Straka, R. Davis-Jones, C. A. Doswell III, F. H. Carr, M. D. Eilts, and D. R. MacGorman, 1994: Verification of the Origins of Rotation in Tornadoes Experiment: VORTEX. *Bull. Amer. Meteor. Soc.,* **75,** 995–1006.

Testud, J., P. H. Hildebrand, and W.-C. Lee, 1995: A procedure to correct airborne Doppler radar data for navigation errors using the echo returned from the earth's surface. *J. Atmos. Oceanic Technol.,* **12,** 800–820.

Wakimoto, R. M., and C. Liu, 1998: The Garden City, Kansas, storm

during the VORTEX 95. Part II: The wall cloud and tornado. *Mon. Wea. Rev.*, **126,** 393–408.
——, and B. L. Bosart, 2000: Airborne radar observations of a cold front during FASTEX. *Mon. Wea. Rev.,* **128,** 2447–2470.
——, W.-C. Lee, H. B. Bluestein, C.-H. Liu, and P. H. Hildebrand, 1996: ELDORA observations during VORTEX 1995. *Bull. Amer. Meteor. Soc.,* **77,** 1465–1481.
——, C. Liu, and H. Cai, 1998: The Garden City, Kansas, storm during the VORTEX 95. Part I: Overview of the storm's lifecycle and mesocyclogenesis. *Mon. Wea. Rev.,* **126,** 372–392.
Webster, P. J., and R. Lukas, 1992: TOGA COARE: The TOGA Coupled Ocean–Atmosphere Response Experiment. *Bull. Amer. Meteor. Soc.,* **73,** 1377–1416.